




## Energy metabolism rewiring following acute UVB irradiation is largely dependent on nuclear DNA damage

Léa Dousset<sup>a,b</sup>, Walid Mahfouf<sup>a</sup>, Hadi Younes<sup>a</sup>, Hala Fatrouni<sup>a</sup>, Corinne Fauchoux<sup>a</sup>, Elodie Muzotte<sup>a</sup>, Ferial Khalife<sup>a</sup>, Rodrigue Rossignol<sup>c,d</sup>, François Moisan<sup>a</sup>, Muriel Cario<sup>a,e</sup>, Stéphane Claverol<sup>f</sup>, Laure Favot-Laforge<sup>g</sup>, Anni I. Nieminen<sup>h</sup>, Seppo Vainio<sup>i</sup>, Nsrein Ali<sup>i</sup>, Hamid-Reza Rezvani<sup>a,e,\*</sup> 

<sup>a</sup> Univ. Bordeaux, Inserm, BRIC, UMR 1312, F-33076, Bordeaux, France

<sup>b</sup> Dermatology Department, Hôpital Saint-André, Bordeaux, France

<sup>c</sup> Univ. Bordeaux, Inserm, MRGM, U1211, Bordeaux, France

<sup>d</sup> CELLOMET, Centre de Génomique Fonctionnelle de Bordeaux, Univ. Bordeaux, Bordeaux, France

<sup>e</sup> Aquiderm, University of Bordeaux, Bordeaux, France

<sup>f</sup> Univ. Bordeaux, Bordeaux Proteome, Bordeaux, France

<sup>g</sup> LIITEC EA 4331, Poitiers, France

<sup>h</sup> FIMM Metabolomics Unit, Institute for Molecular Medicine Finland, University of Helsinki, 00014, Finland

<sup>i</sup> Faculty of Biochemistry and Molecular Medicine, Disease Networks Research Unit, University of Oulu, Oulu, Finland

### ABSTRACT

Solar ultraviolet B (UVB) radiation-induced DNA damage is a well-known initiator of skin carcinomas. The UVB-induced DNA damage response (DDR) involves series of signaling cascades that are activated to maintain cell integrity. Among the different biological processes, little is known about the role of energy metabolism in the DDR.

We sought to determine whether UVB-induced nuclear and/or mitochondrial cyclobutane pyrimidine dimers (CPDs) alter cellular energy metabolism. To gain insight into this question, we took advantage of keratinocytes expressing nuclear or mitochondrial CPD photolyase. Applying a quantitative proteomic approach and targeted metabolomics, we observed biphasic alterations in multiple metabolic pathways and in the abundance of various metabolites, largely influenced by the presence of genomic CPDs. The heightened oxygen consumption rate post-irradiation, along with mitochondrial structural rearrangements, was found to be dependent on both mitochondrial and nuclear CPDs.

Understanding the influence of nuclear and mitochondrial DNA damage on keratinocyte responses to UVB irradiation deepens current knowledge regarding skin cancer prevention, initiation, and therapy.

### 1. Introduction

Solar ultraviolet (UV) radiation is the main risk factor for development of non-melanoma skin cancers (NMSCs), the most common type of human malignancy worldwide. The incidence of NMSCs including basal cell carcinomas and cutaneous squamous cell carcinomas (cSCCs) is increasing by 5–7% per year, mainly due to UV exposure and the ageing of the population [1]. In 2012, 3.3 million patients in the USA were affected [2].

Solar radiation affects skin homeostasis through the induction of well-defined structural alterations in DNA, which in turn, triggers the DNA damage response (DDR) network. The DDR involves sensing damage and subsequently signaling to downstream effectors. The

balance between different activated signaling pathways, which is dependent on the type and extent of the damage and DNA repair capacity, ultimately determines whether a cell remains quiescent, proliferates, differentiates, or undergoes apoptosis [3,4]. The major DNA damage induced by UVB irradiation include cyclobutane pyrimidine dimers (CPDs) and 6–4 photoproducts (6-4 PPs). These lesions are mainly repaired by the nucleotide excision repair (NER) DNA system through the release of a 24-mer to 32-mer oligonucleotide containing the damage and its replacement by a newly synthesized DNA fragment [5].

Characterizing and understanding the molecular basis underlying the cross-talk among different programs forming part of the DDR network are currently the subject of intense investigation. A growing

\* Corresponding author. INSERM U1312, Bordeaux, F-33000, France.

E-mail address: [hamid-reza.rezvani@u-bordeaux.fr](mailto:hamid-reza.rezvani@u-bordeaux.fr) (H.-R. Rezvani).

<https://doi.org/10.1016/j.freeradbiomed.2024.12.030>

Received 21 August 2024; Received in revised form 4 December 2024; Accepted 9 December 2024

Available online 10 December 2024

0891-5849/© 2024 The Authors. Published by Elsevier Inc. This is an open access article under the CC BY license (<http://creativecommons.org/licenses/by/4.0/>).

body of literature suggests that there may be crosstalk between the DDR network and energy metabolism. Therefore, the main aim of this study was to determine whether reprogramming of metabolic pathways also occurs after acute UVB irradiation. If so, the two following scenarios should be taken into account. First, reprogramming of metabolic pathways is an adaptive response and, therefore, reprogramming could be considered as a sub-program of the DDR network supporting the homeostasis of stressed cells. Second, energy metabolism alterations occur prior to DDR activation and therefore play decisive roles in launching and orchestrating the DDR network. The former scenario is supported by evidence showing that sensors (e.g. PARP1), transducers (e.g. ATM), and effectors (e.g. p53, CDK) of the DDR network activate numerous enzymes involved in energy metabolism [6–9]. Evidence for the second scenario comes from data showing that different genotoxic-induced DNA damage results in the early activation of numerous enzymes involved in energy metabolism (such as AMPK, HIF-1, and TIGAR). These metabolic enzymes function as important regulators of diverse cellular processes, including transcriptional regulation, the cell cycle, senescence, apoptosis, and autophagy [9–11]. Moreover, we and others have shown that modifying key regulators of energy metabolism (such as HIF-1 $\alpha$  and Tfam) can impact the repair efficiency of UVB-induced DNA damage [12–14] epidermal differentiation and hair growth [15–20], suggesting that energy metabolism may influence various cellular processes in the skin.

To unravel the role of metabolism in keratinocyte responses to acute UVB irradiation, we took advantage of keratinocytes expressing nuclear or mitochondrial CPD photolyase (Nu-PL and Mt-PL, respectively). We showed here that exposure of keratinocytes to acute UVB light leads to biphasic alterations in numerous metabolic pathways, which are largely dependent on nuclear CPDs and independent of mitochondrial CPDs. The abundance of numerous metabolites in keratinocytes exposed to UVB irradiation also changes in a biphasic manner, and is partially restored in Nu-PL cells. The presence of nuclear and mitochondrial CPDs also affects the structure of the mitochondrial network.

Taken together, the current data provide substantial insights into the links between UVB-induced DNA damage and metabolic alterations in orchestrating DDR network.

## 2. Materials and methods

### 2.1. KHAT cell line and culture media

Human keratinocytes were isolated from normal human skin in patients undergoing plastic surgery and grown in keratinocyte serum-free medium (KSFM) supplemented with 50  $\mu$ g/mL bovine pituitary extract and 0,5 ng/mL epidermal growth factor (Gibco; Thermo Fisher Scientific) in a humidified atmosphere of 5 % CO<sub>2</sub> at 37 °C. The KHAT cell line was generated through immortalization of human primary keratinocytes following transduction with a lentiviral vector expressing hTERT and a large tumor antigen (also called large T-antigen). Transduced keratinocytes were cultivated in parallel with the non-transduced cells in KSFM. Immortalization was considered to occur when KHAT cells grew for 50 population doublings beyond the life span of the parental keratinocytes. These immortalized cells formed a normally stratified epidermis when used in organotypic culture (Fig. S1A). KHAT cells can also form pigmented epidermis when human primary melanocytes are incorporated in skin equivalents (Fig. S1B). The human keratinocytes utilized in this study were obtained with the consent of the patients from surgical excision skin biopsies collected from post-routine medical procedures performed for therapeutic purposes. The collection and use of these biopsies were conducted in strict accordance with Article L. 1243-3 of the French Code of Public Health, under the agreement DC-2008-412 with the University Hospital Center of Bordeaux, France.

### 2.2. UVB irradiation procedure

KHAT cells were irradiated at a dose of 15 mJ.cm<sup>-2</sup> using a Biotronic device (Vilber Lourmat, Marne la Vallée, France), equipped with a dosimeter, in which the UVB lamp emitted a continuous band between 280 and 380 nm (major peak at 312 nm), as previously described [21]. To determine the optimal dose, a propidium iodide (PI) exclusion assay was initially performed to evaluate the viability of keratinocytes following irradiation at different doses. The viability of irradiated keratinocytes was approximately 70 % compared with that of the non-irradiated controls 24 h after irradiation at a dose of 15 mJ.cm<sup>-2</sup> (Fig. S1). This dose was selected for further experiments. For photo-activation of CPD photolyase after irradiation, the cells were incubated for 30 min under 450 nm blue light in a 37 °C 5 % CO<sub>2</sub> incubator.

### 2.3. Western blot procedure

Western blotting was performed as previously described [22]. Briefly, equal amounts of total protein were resolved by SDS-polyacrylamide gel electrophoresis (SDS-PAGE) and electrophoretically transferred to nitocellulose membrane for AMPK and p-AMPK; and to a PDVF membrane for OXPHOS. The membranes were then incubated overnight at 4 °C with primary antibodies (Table 1). After additional incubation with a 1:1000 dilution of an anti-immunoglobulin horse-radish peroxidase-linked antibody (Vector Laboratories, Biovalley S.A., Marne la Vallée, France) for 1 h, blots were developed using the chemiluminescence ECL reagent (Bio-Rad).

### 2.4. Statistics

Comparisons between two groups were performed using Student's t-test (two-tailed), and a p value < 0.05 (\*) was considered to indicate statistical significance. The results were presented as the means  $\pm$  SEM. Comparisons between more than two groups were performed with one-way analysis of variance (ANOVA) followed by Bonferroni's multiple comparison test if the values normally distributed (Shapiro and Wilk test). If the data were not normally distributed, a nonparametric Kruskal-Wallis test associated with Dunn's multiple comparison test was performed. If two independent variables needed to be tested, two-way ANOVA followed by a post hoc Bonferroni correction was used. If the distribution did not follow normality, a mixed-effects model followed by Bonferroni correction was used for multiple comparisons. A p value < 0.05 was considered to indicate statistical significance. The results are presented as the means  $\pm$  SEMs. PCA was performed using GraphPad Prism software.

Additional materials and methods details are found in Supplementary materials and methods.

**Table 1**  
List of antibodies used in this study.

Protein	Reference	Dilution
B-Actine	A2228 - Sigma	1/5000
Tubulin	ab7291	1/5000
OXPHOS tot	ab110411	1/500
Fis-1	Sc-376469	1/500
p-AMPK	Sc101630	1/1000
AMPK	Sc25792	1/1000
LC3B	Cell-Signaling - 38685	1/1000
Cleaved Caspase-3	Cell-Signaling- 9664L	1/1000
TOM20	Sc-17764	1/100
Alexa Fluor™ 488 Phalloidin	Invitrogen-A12379	1/500
Atto 647N	Sigma-50185	1/500

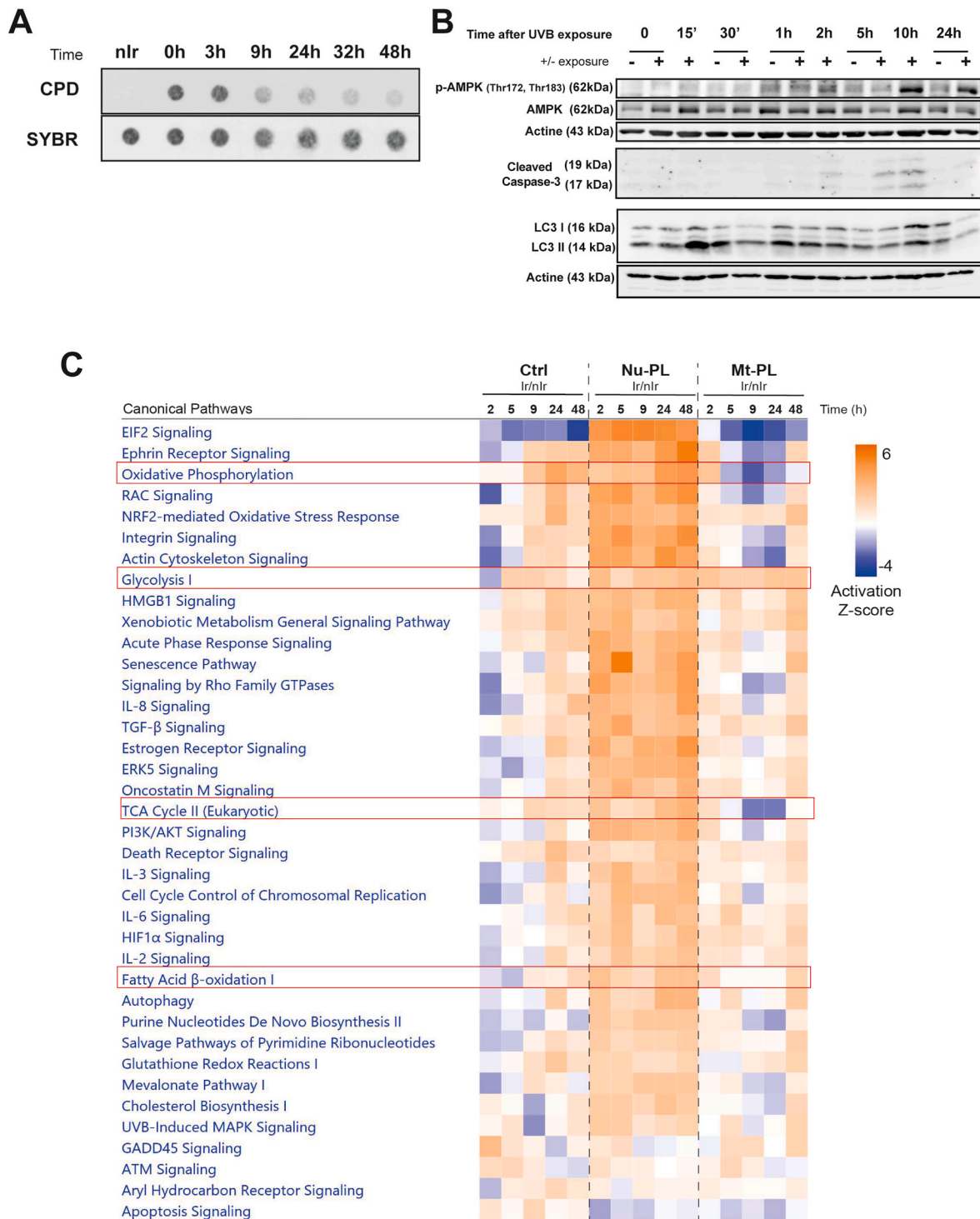


**Fig. 1.** Quantitative proteomic analyses revealed biphasic variations in the activities of several signaling pathways following UVB irradiation. **A**) Cyclopyrimidine dimer (CPD) levels were quantified in the KHAT cell line by immuno-dot blot analysis at different time points after irradiation **B**) The expression levels of AMPK, cleaved caspase-3 and LC3 were analyzed via western blotting. β-Actin was used as a loading control. **C**) Ctrl, Nu-PL and Mt-PL keratinocytes were exposed to acute UVB irradiation. The cells were then harvested at the indicated time points after UV treatment and subjected to label-free quantitative proteome analysis. Heatmap of the z-scores for activated canonical pathways at different hours after acute irradiation, n = 3 per condition. The color indicates canonical pathway activation z-scores; blue: downregulated and orange: upregulated. Nu-PL: keratinocytes expressing nuclear CPD photolyase, Mt-PL: keratinocytes expressing mitochondrial CPD photolyase. (For interpretation of the references to color in this figure legend, the reader is referred to the Web version of this article.)

### 3. Results

#### 3.1. Biphasic variations in energy metabolism pathways induced by UVB irradiation

To study the crosstalk between different programs of the DDR network and metabolism following acute UVB irradiation, we used immortalized human keratinocytes called KHAT. Even though they are immortal, they still retain the ability to form a fully stratified epidermis when used in an organotypic culture (Fig. S1). These keratinocytes were irradiated with a single dose of UVB (15 mJ.cm<sup>-2</sup>). The CPD level was first analyzed at different time points after irradiation using immune-dot blotting (Fig. 1A). The results showed a gradual removal of CPD with a peak between 3 h and 9 h. In addition to the DNA repair machinery, other DDR signaling pathways, such as apoptosis (activated caspase 3 expression), were also triggered in these cells, as shown by western blotting (Fig. 1B). Metabolic sensors, such as AMPK were activated at 10 h and 24 h after acute UVB irradiation (Fig. 1B). To obtain a global overview of signaling pathways triggered by a single exposure to UVB irradiation, we performed a quantitative label-free differential proteomic analysis of samples at different time points after UVB irradiation. Ingenuity Computational Pathway Analysis (IPA®) software ([www.ingenuity.com](http://www.ingenuity.com)) was used to elucidate the global implications of the differentially expressed proteins (DEPs) as well as the potentially modified molecular pathways at different time points after irradiation. First of all, the modified canonical pathways have been identified by applying Z-score >2 as the threshold of significant activation. Indeed, the Z-score activation for a canonical pathway is calculated by considering the expression levels of DEPs related to that pathway in our proteomics dataset, as well as the causal relationships with other proteins in the pathway (i.e., activation and inhibition interactions based on literature findings). This Z-score algorithm also predicts the end-point functions of the pathway. For example, IPA indicated an upregulation of “death receptor signaling” at 24 h post-irradiation compared to non-irradiated cells by considering the changes in 36 proteins in our proteomic data (Fig. S2). The top enriched canonical pathways identified via IPA are shown in Fig. 1C. As expected, numerous well-known signaling pathways, such as the EIF2 signaling pathway, integrin signaling pathway, senescence pathway, death receptor signaling pathway, cell cycle control pathway and ATM signaling pathway, which classically contribute to the DDR programs, are among the enriched canonical pathways. Notably, as shown in the Ctrl column, the majority of these signaling pathways were modified in a biphasic manner, with early down-regulation followed by late upregulation (Fig. 1C).

Besides those pathways, we found that the metabolic pathways involved in energy metabolism, such as oxidative phosphorylation (OXPHOS), glycolysis, the TCA cycle and fatty acid  $\beta$ -oxidation, were also modified in a time-dependent manner (Fig. 1C). Examining the expression levels of proteins implicated in glycolysis, the TCA cycle, and OXPHOS, we observed a significant decrease in the relative expression of several of these proteins at 2 h post-irradiation. However, the expression of several of these proteins was subsequently restored in the following hours (Fig. 2A–C). Regarding OXPHOS, it is important to distinguish between the predictions made by IPA and the up- or down-regulation observed in our proteomic data, as indicated by the color coding in Fig. 2C. This indicates that the reprogramming of metabolic pathways serves as an adaptive response and could be considered a sub-program of the DDR network. Finally, proteins differentially expressed 2 h after irradiation were categorized according to related diseases and biological functions by IPA enrichment analysis. The top enriched gene ontology terms for diseases and biological functions with a p value less than 10<sup>-15</sup> are listed in Fig. 2D. Metabolic diseases were found among this list with a p-value less than 10<sup>-30</sup> (Fig. 2D).

Experiments were also performed on the HaCat keratinocyte cell line. The results revealed biphasic changes in the majority of canonical pathways and in the expression levels of proteins involved in OXPHOS,

similar to our findings in KHAT cells but with differing kinetics (Fig. S3). Hereinafter only the results obtained with KHAT are shown.

Regulation of energy metabolism rewiring by nuclear and mitochondrial DNA damage following acute UVB irradiation.

To determine whether the presence of nuclear and/or mitochondrial CPDs plays a decisive role in launching UVB-induced metabolic alterations, KHAT keratinocytes were transduced with lentiviral vectors expressing nuclear or mitochondrial CPD photolyase (Nu-PL and Mt-PL, respectively) (Fig. S4A). Of note, CPD photolyases are DNA repair enzymes that efficiently remove CPD lesions from DNA. These enzymes require blue light (400–500 nm) as a source of energy to efficiently repair CPD lesions [23,24]. Measurement of the CPD levels indicated that the majority of the CPDs were removed from genomic DNA within 30 min after irradiation in Nu-PL cells, while the repair kinetics of the CPDs in Mt-PL cells were very similar to those in their control counterparts (Fig. S4B). The evaluation of CPD removal from mitochondrial DNA (mtDNA) showed that most CPDs were rapidly removed from the mtDNA of Mt-PL cells. In contrast, the removal kinetics of CPDs from mtDNA in Nu-PL cells were very similar to those observed in the control cells (Fig. S4C).

Focusing on proteomic data, we found that biphasic modifications in canonical pathways observed in control KHAT were largely restored in Nu-PL cells, with no significant alterations detected in the latter (Fig. 1C). On the contrary, biphasic changes in the activity of canonical pathways persisted in Mt-PL cells and were characterized by an initial decrease between 5 and 9 h after acute UVB exposure, followed by a late increase (Fig. 1C). Of note, we observed a delayed restoration in the activities of canonical pathways when comparing the Ctrl and Mt-PL cells.

In accordance with earlier results, no significant decreases were observed in the expression levels of proteins involved in glycolysis, the TCA cycle, or OXPHOS in Nu-PL cells at various time points after irradiation (Fig. 2A–C). In contrast, the expression levels of proteins involved in TCA pathway were lower in irradiated Mt-PL cells than in their non-irradiated counterparts, and the majority of these decreases were persisted for up to 48 h after irradiation (Fig. 2A–C). Moreover, the prediction made by IPA for OXPHOS indicated that the expression of proteins involved in OXPHOS, particularly those associated with complexes III and IV, remains consistently downregulated in Mt-PL cells for at least 48 h post-irradiation (Fig. 2C).

Altogether, our results suggest that UVB irradiation triggers biphasic changes in metabolic pathways associated with energy metabolism, with this response predominantly reliant on UVB-induced damage to nuclear DNA.

#### 3.2. Biphasic variations in the relative abundance of metabolites following acute UVB irradiation

To further examine the effects of acute UVB irradiation on metabolic signatures, KHAT keratinocytes (Ctrl, Nu-PL and Mt-PL) harvested at different time points after UVB irradiation were subjected to metabolomics. Focusing on Ctrl KHAT cells, the results revealed time-dependent alterations in the abundance of metabolites. Based on the kinetics of changes in their expression levels and utilizing K-means clustering (Fig. 3B) and principal component analyses (Fig. 3C), the metabolites were classified into two distinct categories (Fig. 3A–C). The abundance of the first group decreased at 5 h and increased at 48 h after irradiation. Glutamine, glutamate, fumarate and malate were among these metabolites (Fig. 3B–G). In the second group, the abundance of metabolites varied in an inverse manner compared to that in the first group; i.e., the abundance of metabolites increased at 5 h after irradiation and decreased in the following hours (Fig. 3A–C). Saturated fatty acids (palmitate and myristic acids) (Fig. 3C, H–I), alpha-ketoglutarate, NADP, uracil, fructose 6 phosphate and phosphoenolpyruvate were among the metabolites of this group (Fig. 3A–C).

The analysis of metabolomics data revealed that the changes in the

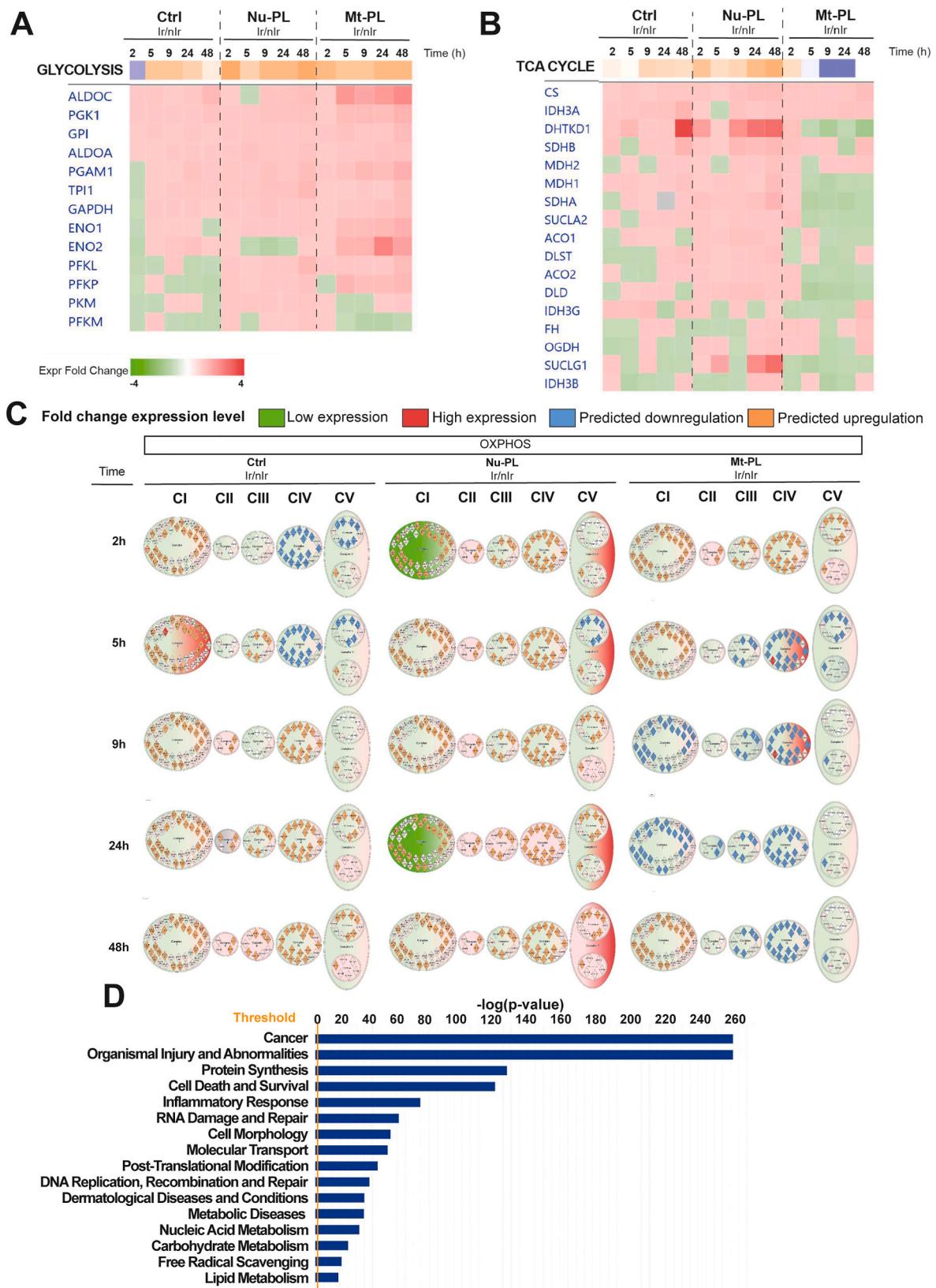


**Fig. 2.** Rapid repair of nuclear and mitochondrial CPDs critically affects the expression patterns of proteins involved in glycolysis, the TCA cycle and OXPHOS (A-C) Proteomic analysis was used to investigate the effects of acute UVB irradiation on the expression profiles of proteins involved in energy metabolism. A heatmap showing the fold change in the expression levels of proteins involved in glycolysis (A), the TCA cycle (B) and OXPHOS (C) at the indicated time points after acute irradiation in the Ctrl, Nu-PL and Mt-PL cells.  $n = 3$  per condition. The color indicates the fold change in the expression level; green: low expression, red: high expression, blue: predicted downregulation, brown: predicted upregulation. D) Gene set enrichment analysis comparing 2 h-postirradiated cells with non-irradiated cells showed that metabolic diseases were among the top 16 enriched Gene Ontology (GO) terms for diseases and biological functions. (For interpretation of the references to color in this figure legend, the reader is referred to the Web version of this article.)

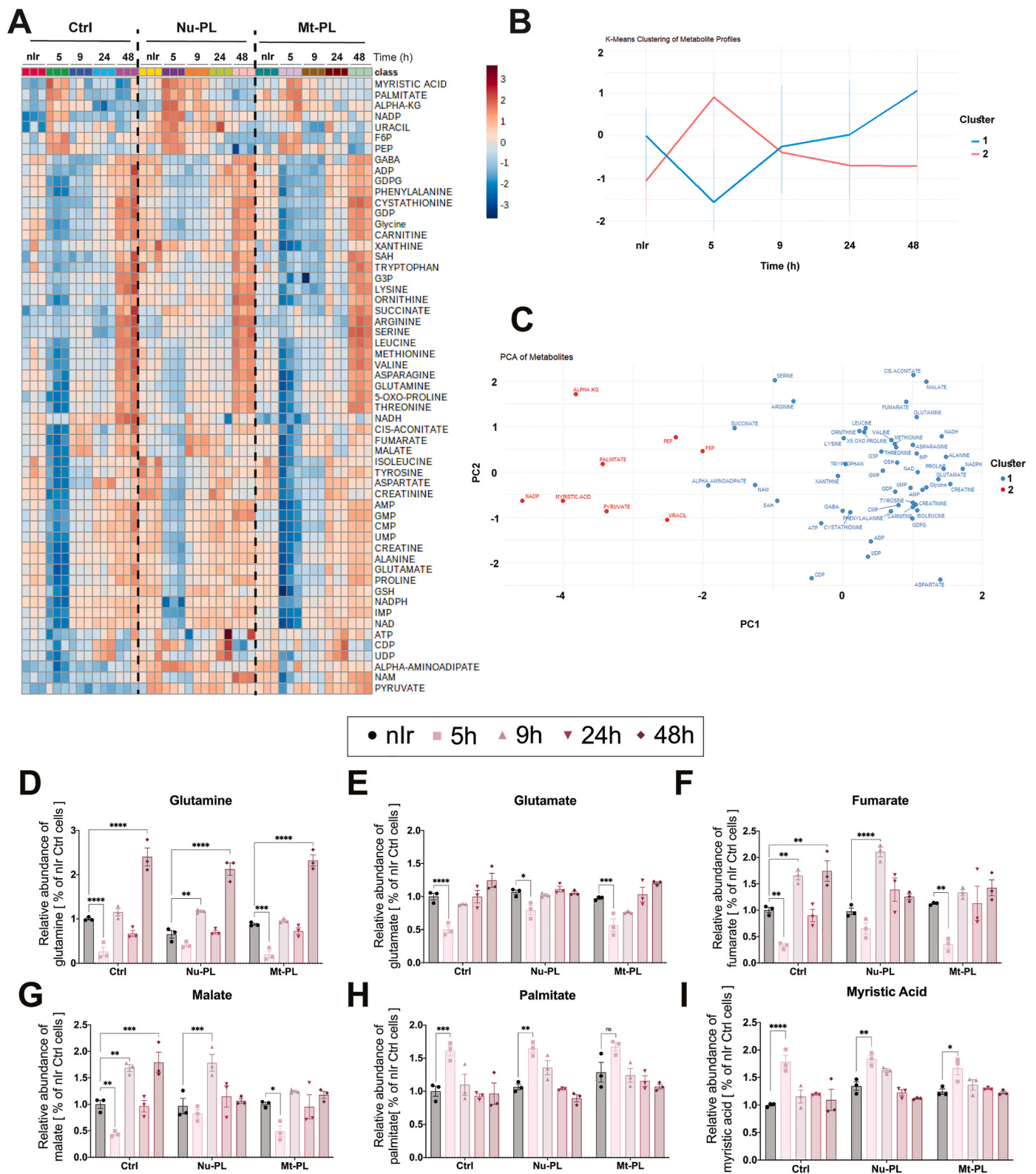


**Fig. 3.** UVB irradiation triggers a biphasic variation in the abundances of metabolites, which is partially dependent on nuclear CPDs. **A)** Ctrl, Nu-PL and Mt-PL keratinocytes were exposed to acute UVB irradiation. The cells were then harvested at the indicated time points after UV treatment and subjected to metabolomics. Heatmap showing the differential abundances of indicated metabolites at different time points after acute UVB irradiation in Ctrl, Nu-PL and Mt-PL cells.  $n = 3$  per condition. The colors indicate low (blue) and high (red) metabolite abundances. **B-C)** K-means clustering (**B**) and PCA (**C**) were applied to classify the metabolites into two groups based on their differential variation patterns following irradiation. **D-I)** Relative abundances of palmitate (**D**), myristic acid (**E**), glutamine (**F**), glutamate (**G**), malate (**H**), fumarate (**I**) were compared at different time points after UVB irradiation in control, Nu-PL and Mt-PL cells. \* $P < 0.05$ , \*\* $< 0.01$  and \*\*\*\* $p < 0.0001$  for irradiated versus the respective non-irradiated cells. (For interpretation of the references to color in this figure legend, the reader is referred to the Web version of this article.)

abundance of metabolites were partially restored in Nu-PL cells exposed to UVB (Fig. 3A). Of note, the primary impact of Nu-PL expression was observed on the first group of metabolites, characterized by marked early downregulation followed by later significant upregulation in both control and Mt-PL cells. Indeed, 5 h after irradiation, no significant downregulation of several of these metabolites was detected in Nu-PL cells, although a tendency toward decreased levels was still observed (Fig. 3A, D–G). The late upregulation of the abundances of the majority of these metabolites was similar among the control, Mt-PL and Nu-PL cells (Fig. 3A, D–G).

Altogether, our results indicate that keratinocytes respond to UVB exposure by altering their metabolic patterns as an adaptive mechanism.

### 3.3. Upregulation of OXPHOS as a late keratinocyte response to UVB irradiation

To further investigate the effects of acute UVB irradiation on energy metabolism, biochemical functional analyses were performed on keratinocytes. While no significant differences were detected in the basal extracellular acidification rate (ECAR) between irradiated cells at either time point (5, 9, or 24 h) and non-irradiated cells (Fig. 4A–C), the glucose-stimulated glycolysis and the maximal glycolytic capacity were significantly greater at 24 h after irradiation than in non-irradiated keratinocytes (Fig. 4D–F). To evaluate OXPHOS activity following irradiation, the basal oxygen consumption rate (OCR) was measured. By comparing non-irradiated and irradiated cells at different time points, we observed a significant increase in both basal OCR and maximal respiratory capacity only at 24 h post-irradiation (Fig. 4G). To further examine the effect of acute UVB irradiation on OXPHOS activity, maximal respiration via different mitochondrial complexes was evaluated. CI- and CII-dependent respiration was modified following UVB irradiation in a biphasic manner (Fig. 4H–I). While no significant modification in the CIII-linked OCR was observed over time (Fig. 4J), a significant increase in the CIV-dependent OCR was detected at 24 h post-irradiation (Fig. 4K). In agreement with these findings, the expression levels of nuclear-encoded mitochondrial complex I's subunit NDUF8B, II's subunit SDHB, III's subunit UQCRC2, and IV's subunit COX II were upregulated in cells at 24 h post-irradiation compared to those in non-irradiated keratinocytes (Fig. 4L).

Biochemical functional analyses revealed that, similarly to those in control cells, glucose-stimulated glycolysis and glycolytic capacity were greater in Nu-PL cells at 24 h post-irradiation than in non-irradiated Nu-PL keratinocytes (Fig. S5A). Although not significantly different, there was a tendency toward increased glucose-stimulated glycolysis and glycolytic capacity in Mt-PL cells at 24 h after irradiation (Fig. S5B). Measurement of oxygen consumption in Nu-PL or Mt-PL cells at 24 h after irradiation indicated that, unlike those in control cells, neither the basal nor uncoupled OCR levels were significantly different from the levels found in their respective non-irradiated counterpart cells (Fig. 4M and N). However, similar to those in control cells, the CI- and CIV-dependent respiration in Nu-PL cells at 24 h after irradiation was higher than that in non-irradiated cells (Fig. S5 C–F). In agreement, the protein expression levels of the mitochondrial subunits tended to increase at 9 and 24 h after irradiation in these cells (Fig. S5G). No significant differences in CI-, CII-, CIII-, or CIV-linked respiration rates were detected between irradiated Mt-PL cells and their respective non-irradiated counterparts (Figs. S5H–K).

Altogether, our data reveal that OXPHOS is upregulated as a late response to UVB irradiation. Both nuclear and mitochondrial DNA damage are pivotal in driving this response.

### 3.4. Dynamic morphological and structural remodeling of the mitochondrial network following UVB exposure

Mitochondrial network morphology is critically linked to bioenergetics, and consequently undergoes changes upon metabolic or

environmental stress[22,25–27]. The morphology of the mitochondrial network is dependent mainly on the balance between mitochondrial fusion and fission. Generally, while mitochondrial fission allows the exclusion of damaged mitochondria, mitochondrial fusion enables the exchange between functional mitochondria [28].

To examine the effect of UVB irradiation on mitochondrial network features, we first wondered whether the mitochondrial DNA content is modified following irradiation. The results indicated that the mtDNA to genomic DNA ratio in the irradiated cells was not significantly different from that in the non-irradiated samples (Fig. 5A). We then examined the morphological and structural remodeling of the mitochondrial network at different time points after UVB irradiation. To this end, the Mito-SegNet model was generated with a training set of 40 1024 × 1024-pixel confocal microscopy images, depicting mitochondria in the body wall of keratinocytes (Fig. 5B and methods). As shown in Fig. 5C, dynamic rearrangement of the mitochondrial network was observed at different time points after irradiation. Principal component analysis (PCA) indicated that the mitochondrial network features in cells at 9 h after irradiation were farthest from those in the other groups (Fig. 6A–D, and Fig. S6). Quantification analysis indicated that the average major axis, minor axis, perimeter and eccentricity of mitochondria increased 9 h after irradiation. In contrast, the average solidity, number of branches and total branch length were diminished in these cells (Fig. 6C), suggesting an increase in fission process at 9 h after irradiation. In agreement, the expression of mitochondrial fission 1 protein (Fis-1) was rapidly upregulated following irradiation. This increase in expression was followed by a decrease 24 h post-irradiation (Fig. 6D).

Overall, our results indicate that mitochondrial network features are dynamically modified at different time points after UVB exposure, as indicated by molecular and morphological evidence of fission.

Mitochondrial network features at different time points after UVB irradiation were ultimately evaluated in Nu-PL and Mt-PL cells and compared with those in control cells. PCA indicated that the mitochondrial network features of irradiated cells at any time point after irradiation were very similar and could not be discriminated from each other in either Nu-PL or Mt-PL cells. However, there were several differences between irradiated and non-irradiated cells under both conditions (Fig. 6E and F). Analyses of cells at 9 h after irradiation indicated that the average major axis, minor axis, and perimeter of mitochondria were lower in irradiated cells than in non-irradiated cells. In contrast, the average solidity was greater in both cells compared to that in their non-irradiated counterpart cells (Fig. 6G and H), suggesting that the mitochondrial fusion process increased after irradiation in these cells.

Collectively, our findings show that both nuclear and mitochondrial CPDs are key regulators of keratinocyte responses to UVB, influencing mitochondrial features (morphology and function) by controlling/synchronizing metabolic protein expression patterns.

## 4. Discussion

Overwhelming evidence indicates that DDR network activation alters the metabolic functions of the host organism, and vice versa, that the metabolic profile of the host regulates DDR [5,29,30]. The reprogramming of metabolic pathways following acute UVB irradiation may reflect either an adaptive response to support the homeostasis of stressed cells or a role as a key organizer of DDR network activation. Distinguishing between these two scenarios is inherently challenging. The presence of nuclear CPDs and the associated cell cycle arrest, along with the increased demand for nucleotide biosynthesis, the repair of other UV-induced damage (such as oxidized proteins and lipids), and the restoration of oxidative balance post-UV irradiation, could all significantly influence metabolic changes. Considering the bidirectional relationship between DDR network activation and metabolic reprogramming, we aimed to study the effect of UVB-induced nuclear and mitochondrial CPDs on the metabolic signatures of keratinocytes. Overall, our results indicated that rapid removal of CPD in Nu-PL cells

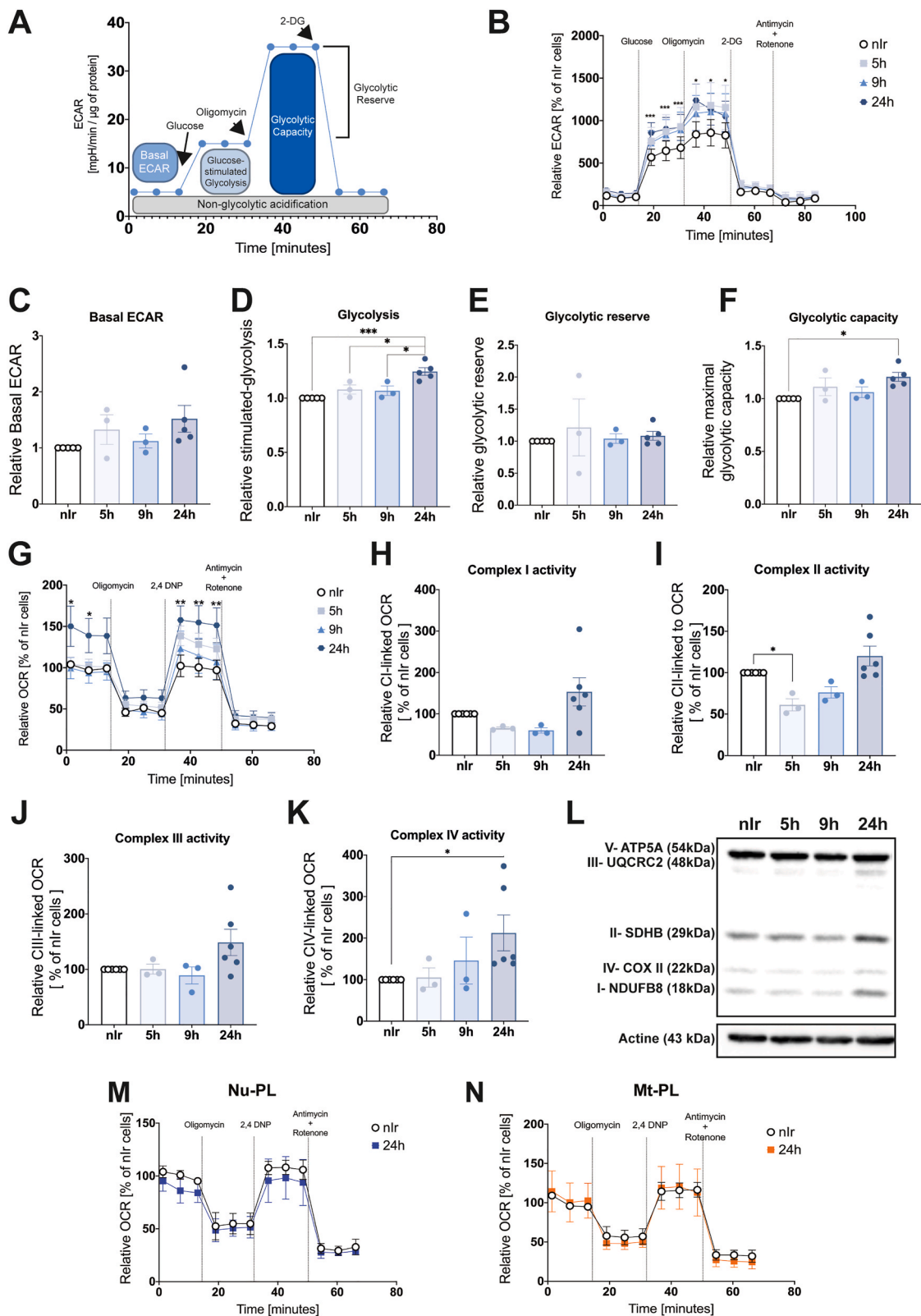


**Fig. 4.** OXPHOS is upregulated at 24 h after acute UVB irradiation **A**) Schematic representation of ECAR kinetics in cell response to glucose, oligomycin and 2-DG. **B-F**) Extracellular acidification (ECAR) **B**) basal ECAR **C**), glucose-stimulated ECAR **D**), glycolytic reserves **E**) and glycolytic capacity **F**) of KHAT at different times after irradiation were measured.  $3 \leq n \leq 7$  [**B-F**], and significant p values ( $<0.05$ ) from the mixed-effect model [**B**], and one way ANOVA [**C-F**]. **G-K**) The oxygen consumption rate (OCR) and mitochondrial complex-linked respiration were measured.  $3 \leq n \leq 7$  [**G-K**] and significant p values ( $<0.05$ ) from the mixed-effect model [**G**], one-way ANOVA [**H-J**], and the Kruskal-Wallis test with  $3 \leq n \leq 7$  [**K**]. **L**) Representative western blot showing the five proteins involved in OXPHOS (ATP5A, ATP synthase alpha subunit; UQCRC2, ubiquinol-cytochrome c reductase core protein II; SDHB, succinate dehydrogenase complex iron sulfur subunit B; COXII, cytochrome c oxidase II; NDUFB8, NADH:ubiquinone oxidoreductase subunit B8.  $\beta$ -Actine was used as a loading control. **M-N**) The OCR was measured in Nu-PL (**J**) and Mt-PL (**K**) cells at different time points after irradiation. p values were calculated by the mixed-effect model.  $n = 4$ .



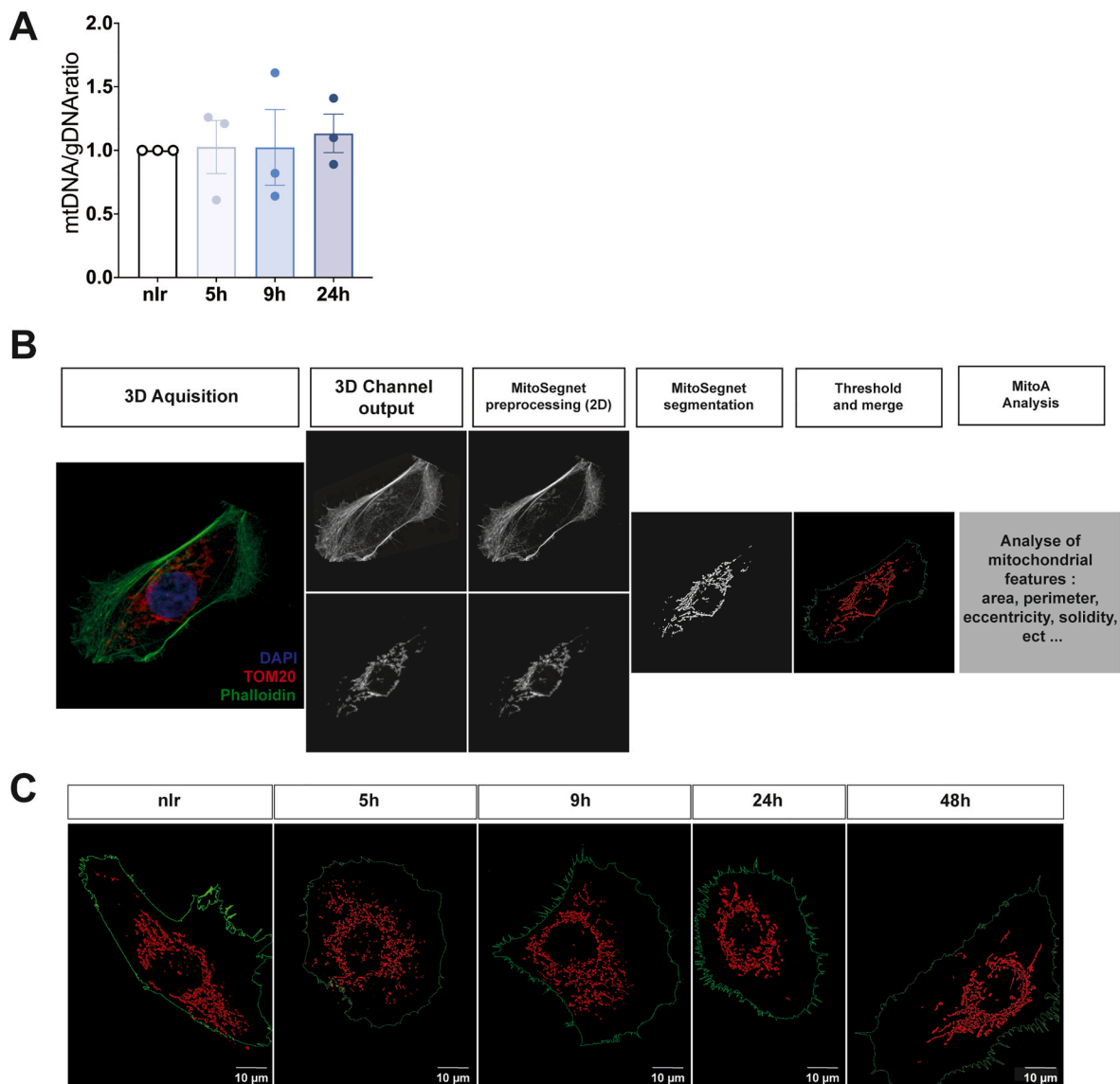


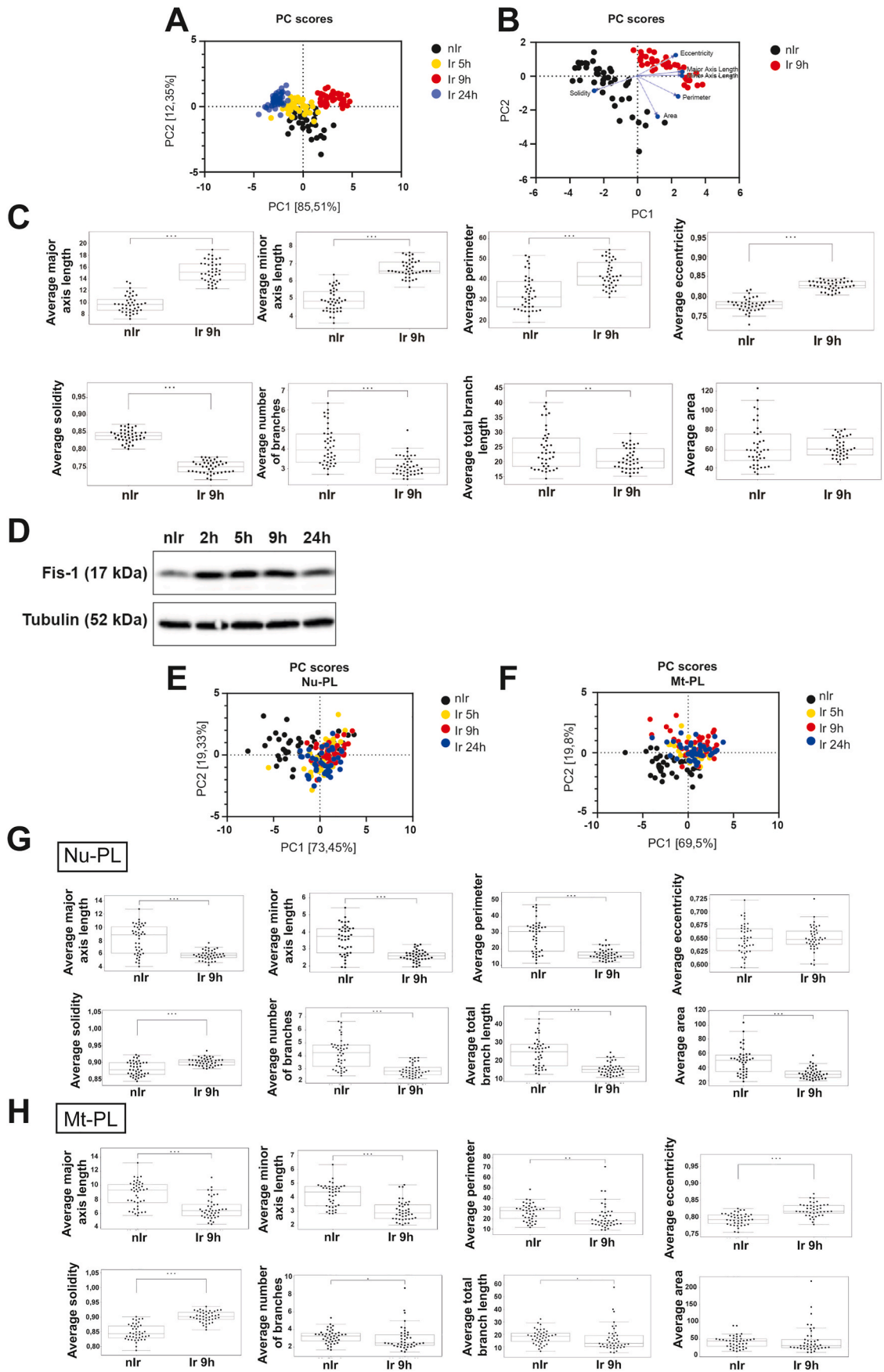
**Fig. 5.** Dynamic modifications in mitochondrial morphology features after UVB irradiation **A**) The mtDNA/gDNA ratio was assessed by qPCR. p value was calculated from the Kruskal-Wallis test.  $n = 3$ . **B**) Schematic representation of image processing by MitoSegNet for quantitative analyses with MitoA software. Mitochondria imaged by confocal microscopy were subjected to image processing, which involved 2D deconvolution, morphological transformation, intensity thresholding, and object quantification. Phalloidin labeled in green was used to determine the thresholding boundaries for each individual cell. **C**) Representative images showing mitochondrial network features at the indicated time points after irradiation. (For interpretation of the references to color in this figure legend, the reader is referred to the Web version of this article.)

restored the early downregulation of canonical pathways; the expression levels of proteins involved in glycolysis, the TCA cycle and OXPHOS; and the early decrease in the abundance of the majority of metabolites. Furthermore, rapid removal of nuclear CPD blocked the UVB-induced mitochondrial fission process observed in UVB-irradiated control cells. Rapid removal of CPDs from mtDNA in Mt-PL cells led to modified patterns of canonical pathway activation, increases in the levels of several metabolites, alterations in mitochondrial-dependent metabolism and changes in mitochondrial network features compared to those in UVB-irradiated control cells. It is worth noting that when comparing Nu-PL and Mt-PL cells to control cells under non-irradiated (baseline) conditions, the activation z-scores for various canonical pathways and the fold changes in proteins involved in glycolysis and the TCA cycle differ among Nu-PL, Mt-PL cells, and the control cells. However, the magnitude of these differences is significantly smaller than the changes observed after irradiation (Fig. S7). Similarly, baseline levels (non-irradiated conditions) of certain metabolites differ among Ctrl, Nu-PL, and

Mt-PL cells (Fig. 3C–J), suggesting that photolyase expression may have specific effects on cellular metabolism. Further investigations are required to elucidate the mechanisms underlying these modifications.

#### 4.1. Metabolism reprogramming upon UVB irradiation

DDR programs are highly energy demanding processes [29,31]. Moreover, several DDR components (such as ATM, p53 and CDK) have been shown to modulate the activities of several enzymes involved in energy metabolism [6–9,29]. Therefore, it is not surprising that genotoxic stress-induced DDR network triggers metabolic alterations. It has been shown that the exposure of HaCat cells to acute UVB irradiation leads to the upregulation of glycolysis, mitochondrial respiration and fatty acid  $\beta$ -oxidation 24 h post-irradiation [32,33]. Similarly, exposure of skin equivalents to UVB has been shown to induce an immediate upregulation of G6PD, the key enzyme initiating glucose metabolism through the oxidative branch of the pentose phosphate pathway (PPP),



(caption on next page)

**Fig. 6.** The effects of nuclear and mitochondrial CPDs on the dynamics of mitochondrial morphology modifications **A–B**) PCA plot comparing mitochondrial morphology features (including solidity, eccentricity, major and minor axis length, area and perimeter) among non-irradiated (nIr) and irradiated (Ir) cells at 5 h, 9 h and 24 h post-irradiation. **C**) Mitochondrial morphology features were compared between Ctrl cells that were not irradiated and those that were 9 h post-irradiation. **D**) Representative western blot showing Fis-1 expression levels at the indicated time points after UVB irradiation. Tubulin was used as a loading control. **E–F**) PCA plot comparing mitochondrial morphology features (including solidity, eccentricity, major and minor axis length, area and perimeter) among non-irradiated (nIr) and irradiated cells at 5 h, 9 h and 24 h post-irradiation in both Nu-PL (**E**) and Mt-PL (**F**) cells. **G–H**) Mitochondrial morphology features were compared between Nu-PL (**G**) and Mt-PL (**H**) cells under non-irradiated condition and 9 h post-irradiation.

across all layers of the epidermis [34]. Activation of the oxidative PPP flux 1) results in an increased NADPH/NADP<sup>+</sup> ratio, thereby enhancing ROS clearance mechanisms, and 2) provides building blocks for de novo nucleotide biosynthesis [35]. Our results showed that most metabolic pathways were altered in a biphasic manner with early downregulation followed by significant upregulation in both examined keratinocyte cell lines (Figs. 1–3 and S3). Therefore, examining cell response kinetics is key to better understanding the essence of the crosstalk between DDR activation and metabolism (i.e., maintenance of cell survival and homeostasis). In agreement, several studies have shown that acute exogenous genotoxic stress-induced DDR represses the expression of enzymes involved in the TCA cycle and OXPHOS at the transcriptional level, typically 1–2 h after exposure [36,37]. However, examination at longer time points revealed a significant increase in the OCR and in the expression levels of genes involved in mitochondrial respiration [38]. Late metabolic modifications likely occur to compensate for the depletion of cellular ATP, NAD<sup>+</sup> and other metabolites during the repair process of DNA damage [32,33,39–41]. Accordingly, the biphasic modulations in metabolic pathways and upregulated mitochondrial respiration 24 h after irradiation were abolished in cells expressing Nu-PL (Figs. 1C and 4M). Moreover, modified metabolism has also been demonstrated in several models of DNA repair-deficient diseases. For example, cells from xeroderma pigmentosum (XP) patients (such as XP-C, XP-D and XP-A patients) and Cockayne syndrome (CS) patients have shown intrinsically altered metabolism, such as increased glycolysis and decreased mitochondrial metabolism [5], indicating that cells in which DNA damage persistently accumulates need to change their metabolism to ensure homeostasis.

#### 4.2. Functional mitochondria in cell responses to UVB irradiation

Owing to its central function in numerous cellular processes including cell cycle progression, apoptosis/senescence and autophagy, energy metabolism plays a crucial role in cellular homeostasis under stress conditions. It is now widely accepted that OXPHOS and glycolysis cooperate to sustain the variable energy demands and anabolic (biosynthetic) needs of cells during their responses to stressors [42,43] and that human cells achieve those needs through various regulatory mechanisms referred to as metabolic reprogramming [44–46]. Besides energy demands, functional mitochondria are also crucial for supporting cellular biosynthetic fluxes, which are necessary for providing cellular building blocks such as nucleic acids, proteins and membranes, but also for redox resetting to acquire a new redox balance upon stress [42,43,47]. Therefore, it is unsurprising that cells with the ability to rapidly remove CPDs from their mtDNA (i.e., Mt-PL cells) exhibit different responses to UVB compared to control cells. Our data indeed revealed significant differences in the activation profiles of canonical pathways and mitochondrial network features following irradiation between Mt-PL and control cells (Figs. 1, 2 and 6). One possible explanation is that persistent mtDNA damage following UVB irradiation can induce mitochondrial dysfunction by promoting mitochondrial ROS generation, as observed in response to other genotoxic insults [48,49]. In addition to the presence of CPD on mtDNA, ROS-mediated mitochondrial dysfunction may contribute to the observed modifications in control cells. In Mt-PL cells, the removal of CPD from mtDNA contributes to the maintenance of mtDNA integrity. However, the persistence of nuclear CPDs on genomic DNA and the consequent reduction in the expression of nuclear-encoded mitochondrial enzymes leads to an imbalance between

mitochondrial-encoded enzymes and nuclear-encoded enzymes. This imbalance could explain the observed delay in the restoration of several detected modifications.

A better understanding of the role of metabolism in keratinocyte responses to UVB is crucial for developing adapted metabolic therapies for the prevention and treatment of skin cancers, as proposed for isocitrate dehydrogenase (IDH) 1 and 2 mutant tumors [50,51] or for oxidative human lung adenocarcinomas [52].

#### CRediT authorship contribution statement

**Léa Dousset:** Writing – review & editing, Writing – original draft, Validation, Methodology, Formal analysis, Data curation. **Walid Mahfouf:** Writing – review & editing, Methodology, Formal analysis, Data curation. **Hadi Younes:** Writing – review & editing, Methodology, Formal analysis, Data curation. **Hala Fatrouni:** Formal analysis, Data curation. **Corinne Faucheux:** Validation, Methodology, Formal analysis, Data curation. **Elodie Muzotte:** Validation, Methodology, Formal analysis, Data curation. **Ferial Khalife:** Writing – review & editing, Data curation. **Rodrigue Rossignol:** Methodology, Conceptualization. **François Moisan:** Methodology, Formal analysis. **Muriel Cario:** Methodology, Formal analysis. **Stéphane Claverol:** Validation, Methodology, Data curation. **Laure Favot-Laforge:** Writing – original draft, Formal analysis, Conceptualization. **Anni I. Nieminen:** Validation, Formal analysis, Data curation. **Seppo Vainio:** Methodology, Formal analysis. **Nsrein Ali:** Writing – original draft, Validation, Formal analysis, Data curation, Conceptualization. **Hamid-Reza Rezvani:** Writing – review & editing, Writing – original draft, Validation, Supervision, Project administration, Funding acquisition, Formal analysis, Data curation, Conceptualization.

#### Data availability

The authors declare that the data supporting the findings of this study are available within the paper and its Supplementary Information files. The mass spectrometry proteomics data have been deposited in the ProteomeXchange Consortium via the PRIDE partner repository with the dataset identifier PXD051736. Additional data are available from the corresponding author upon reasonable request.

#### Declaration of competing interest

The authors declare that they have no known competing financial interests or personal relationships that could have appeared to influence the work reported in this paper.

#### Acknowledgments

The authors wish to thank Véronique Guyonnet-Duperat (TBMCore, Plateforme de Vectorologie, University of Bordeaux), Aquiderm for providing YSI. Funding: H.R.R gratefully acknowledges support from the Institut National du Cancer “INCa 2021-105”, the PNREST Anses (The French National Research Program for Environmental and Occupational Health of Anses (ANSES-2022-RF-008), and “Société Française de Dermatologie (SFD). FIMM metabolomics unit was supported by the Helsinki Institute of Life Science (HiLIFE) and Biocenter Finland.

## Appendix A. Supplementary data

Supplementary data to this article can be found online at <https://doi.org/10.1016/j.freeradbiomed.2024.12.030>.

## References

- [1] M.R. Donaldson, B.M. Coldiron, No end in sight: the skin cancer epidemic continues, *Semin. Cutan. Med. Surg.* (2011), <https://doi.org/10.1016/j.sder.2011.01.002>.
- [2] H.W. Rogers, M.A. Weinstock, S.R. Feldman, B.M. Coldiron, Incidence estimate of nonmelanoma skin cancer (keratinocyte carcinomas) in the us population, *JAMA Dermatol.* (2015), <https://doi.org/10.1001/jamadermatol.2015.1187>.
- [3] A. Bouafia, S. Corre, D. Gilot, N. Mouchet, S. Prince, M.D. Galibert, p53 requires the stress sensor USF1 to direct appropriate cell fate decision, *PLoS Genet.* (2014), <https://doi.org/10.1371/journal.pgen.1004309>.
- [4] O. Surova, B. Zhivotovsky, Various modes of cell death induced by DNA damage, *Oncogene* (2013), <https://doi.org/10.1038/ncr.2012.556>.
- [5] M. Hosseini, K. Ezzedine, A. Taieb, H.R. Rezvani, Oxidative and energy metabolism as potential clues for clinical heterogeneity in nucleotide excision repair disorders, *J. Invest. Dermatol.* (2015), <https://doi.org/10.1038/jid.2014.365>.
- [6] A. Alexander, J. Kim, C.L. Walker, ATM engages the TSC2/mTORC1 signaling node to regulate autophagy, *Autophagy* (2010), <https://doi.org/10.4161/auto.6.5.12509>.
- [7] E.F. Fang, M. Scheibye-Knudsen, K.F. Chua, M.P. Mattson, D.L. Croteau, V.A. Bohr, Nuclear DNA damage signalling to mitochondria in ageing, *Nat. Rev. Mol. Cell Biol.* (2016), <https://doi.org/10.1038/nrm.2016.14>.
- [8] J. Liu, C. Zhang, W. Hu, Z. Feng, Tumor suppressor p53 and its mutants in cancer metabolism, *Cancer Lett.* (2015), <https://doi.org/10.1016/j.canlet.2013.12.025>.
- [9] T. Sanli, G.R. Steinberg, G. Singh, T. Tsakiridis, AMP-activated protein kinase (AMPK) beyond metabolism: a novel genomic stress sensor participating in the DNA damage response pathway, *Cancer Biol. Ther.* (2014), <https://doi.org/10.4161/cbt.26726>.
- [10] C. Ji, B. Yang, Y.L. Yang, S.H. He, D.S. Miao, L. He, Z.G. Bi, Exogenous cell-permeable C6 ceramide sensitizes multiple cancer cell lines to Doxorubicin-induced apoptosis by promoting AMPK activation and mTORC1 inhibition, *Oncogene* (2010), <https://doi.org/10.1038/ncr.2010.379>.
- [11] J. Obacz, S. Pastorekova, B. Vojtesek, R. Hrstka, Cross-talk between HIF and p53 as mediators of molecular responses to physiological and genotoxic stresses, *Mol. Cancer* (2013), <https://doi.org/10.1186/1476-4598-12-93>.
- [12] W. Mahfouf, M. Hosseini, E. Muzotte, M. Serrano-Sanchez, L. Dousset, F. Moisan, W. Rachidi, A. Taieb, J. Rudolf, H.R. Rezvani, Loss of epidermal HIF-1 $\alpha$  blocks UVB-induced tumorigenesis by affecting DNA repair capacity and oxidative stress, *J. Invest. Dermatol.* 139 (2019) 2016–2028.e7, <https://doi.org/10.1016/j.jid.2019.01.035>.
- [13] H.R. Rezvani, W. Mahfouf, N. Ali, C. Chemin, C. Ged, A.L. Kim, H. de Verneuil, A. Taieb, D.R. Bickers, F. Mazurier, Hypoxia-inducible factor-1 $\alpha$  regulates the expression of nucleotide excision repair proteins in keratinocytes, *Nucleic Acids Res.* 38 (2010) 797–809, <https://doi.org/10.1093/nar/gkp1072>.
- [14] H.R. Rezvani, S. Dedieu, S. North, F. Belloc, R. Rossignol, T. Letellier, H. De Verneuil, A. Taieb, F. Mazurier, Hypoxia-inducible factor-1 $\alpha$ , a key factor in the keratinocyte response to UVB exposure, *J. Biol. Chem.* 282 (2007) 16413–16422, <https://doi.org/10.1074/jbc.M611397200>.
- [15] R.B. Hamanaka, N.S. Chandel, Mitochondrial metabolism as a regulator of keratinocyte differentiation, *Cell. Logist.* (2013), <https://doi.org/10.4161/cl.25456>.
- [16] R.B. Hamanaka, A. Glasauer, P. Hoover, S. Yang, H. Blatt, A.R. Mullen, S. Getsios, C.J. Gottardi, R.J. DeBerardinis, R.M. Lavker, N.S. Chandel, Mitochondrial reactive oxygen species promote epidermal differentiation and hair follicle development, *Sci. Signal.* (2013), <https://doi.org/10.1126/scisignal.2003638>.
- [17] W.J. Wong, T. Richardson, J.T. Seykora, G. Cotsarelis, M.C. Simon, Hypoxia-inducible factors regulate filaggrin expression and epidermal barrier function, *J. Invest. Dermatol.* (2015), <https://doi.org/10.1038/jid.2014.283>.
- [18] J.E. Kloepper, O.R. Baris, K. Reuter, K. Kobayashi, D. Weiland, S. Vidali, D.J. Tobin, C. Niemann, R.J. Wiesner, R. Paus, Mitochondrial function in murine skin epithelium is crucial for hair follicle morphogenesis and epithelial-mesenchymal interactions, *J. Invest. Dermatol.* (2015), <https://doi.org/10.1038/jid.2014.475>.
- [19] O.R. Baris, A. Klose, J.E. Kloepper, D. Weiland, J.F.G. Neuhaus, M. Schauen, A. Wille, A. Müller, C. Merkwirth, T. Langer, N.G. Larsson, T. Krieg, D.J. Tobin, R. Paus, R.J. Wiesner, The mitochondrial electron transport chain is dispensable for proliferation and differentiation of epidermal progenitor cells, *Stem Cell.* (2011), <https://doi.org/10.1002/stem.695>.
- [20] H.R. Rezvani, N. Ali, M. Serrano-Sanchez, P. Dubus, C. Varon, C. Ged, C. Pain, M. Cario-André, J. Seneschal, A. Taieb, H. de Verneuil, F. Mazurier, Loss of epidermal hypoxia-inducible factor-1 $\alpha$  accelerates epidermal aging and affects re-epithelialization in human and mouse, *J. Cell Sci.* (2011), <https://doi.org/10.1242/jcs.082370>.
- [21] H.R. Rezvani, F. Mazurier, M. Cario-André, C. Pain, C. Ged, A. Taieb, H. De Verneuil, Protective effects of catalase overexpression on UVB-induced apoptosis in normal human keratinocytes, *J. Biol. Chem.* (2006), <https://doi.org/10.1074/jbc.M600536200>.
- [22] H.R. Rezvani, A.L. Kim, R. Rossignol, N. Ali, M. Daly, W. Mahfouf, N. Bellance, A. Taieb, H. De Verneuil, F. Mazurier, D.R. Bickers, XPC silencing in normal human keratinocytes triggers metabolic alterations that drive the formation of squamous cell carcinomas, *J. Clin. Invest.* (2011), <https://doi.org/10.1172/JCI40087>.
- [23] L.O. Essen, T. Klar, Light-driven DNA repair by photolyases, *Cell. Mol. Life Sci.* (2006), <https://doi.org/10.1007/s00018-005-5447-y>.
- [24] G.B. Sancar, A. Sancar, Purification and characterization of DNA photolyases, *Methods Enzymol.* (2006), [https://doi.org/10.1016/S0076-6879\(06\)08009-8](https://doi.org/10.1016/S0076-6879(06)08009-8).
- [25] D. Tondera, S. Grandemange, A. Jourdain, M. Karbowski, Y. Mattenberger, S. Herzog, S. Da Cruz, P. Clerc, I. Raschke, C. Merkwirth, S. Ehse, F. Krause, D. C. Chan, C. Alexander, C. Bauer, R. Youle, T. Langer, J.-C. Martinou, SLP-2 is required for stress-induced mitochondrial hyperfusion, *EMBO J.* 28 (2009) 1589–1600, <https://doi.org/10.1038/emboj.2009.89>.
- [26] S.G. Rolland, E. Motori, N. Memar, J. Hensch, S. Frank, K.F. Winkhofer, B. Conradt, Impaired complex IV activity in response to loss of LRPPRC function can be compensated by mitochondrial hyperfusion, *Proc. Natl. Acad. Sci. U.S.A.* (2013), <https://doi.org/10.1073/pnas.1303872110>.
- [27] T. Wai, T. Langer, Mitochondrial dynamics and metabolic regulation, *Trends Endocrinol. Metabol.* (2016), <https://doi.org/10.1016/j.tem.2015.12.001>.
- [28] L. Pernas, L. Scorrano, Mito-morphosis: mitochondrial fusion, fission, and cristae remodeling as key mediators of cellular function, *Annu. Rev. Physiol.* (2016), <https://doi.org/10.1146/annurev-physiol-021115-105011>.
- [29] D. Cucchi, A. Gibson, S.a. Martin, The emerging relationship between metabolism and DNA repair, *Cell Cycle* (2021), <https://doi.org/10.1080/15384101.2021.1912889>.
- [30] M. Hosseini, Z. Kasraian, H.R. Rezvani, Energy metabolism in skin cancers: a therapeutic perspective, *Biochim. Biophys. Acta Bioenerg.* 1858 (2017) 712–722, <https://doi.org/10.1016/j.bbabi.2017.01.013>.
- [31] A. Kaniak-Golik, A. Skoneczna, Mitochondria-nucleus network for genome stability, *Free Radic. Biol. Med.* (2015), <https://doi.org/10.1016/j.freeradbiomed.2015.01.013>.
- [32] C. Hegedűs, T. Juhász, E. Fidrus, E.A. Janka, G. Juhász, G. Boros, G. Paragh, K. Uray, G. Emri, É. Remenyik, P. Bai, Cyclobutane pyrimidine dimers from UVB exposure induce a hypermetabolic state in keratinocytes via mitochondrial oxidative stress, *Redox Biol.* 38 (2021) 101808, <https://doi.org/10.1016/j.redox.2020.101808>.
- [33] C. Hegedűs, G. Boros, E. Fidrus, G.N. Kis, M. Antal, T. Juhász, E.A. Janka, L. Jankó, G. Paragh, G. Emri, P. Bai, É. Remenyik, PARP1 inhibition augments UVB-mediated mitochondrial changes—implications for UV-induced DNA repair and photocarcinogenesis, *Cancers* (2020), <https://doi.org/10.3390/cancers12010005>.
- [34] J.L. Kremer, G.P. Melo, P.C. Marinello, H.P. Bordini, A.C. Rossaneis, L.R. Sábio, R. Cecchini, A.L. Cecchini, W.A. Verri, R.C. Luiz, Citral prevents UVB-induced skin carcinogenesis in hairless mice, *J. Photochem. Photobiol. B Biol.* (2019), <https://doi.org/10.1016/j.jphotobiol.2019.111565>.
- [35] A. Kuehne, H. Emmert, J. Soehle, M. Winnefeld, F. Fischer, H. Wenck, S. Gallinat, L. Terstegen, R. Lucius, J. Hildebrand, N. Zamboni, Acute activation of oxidative pentose phosphate pathway as first-line response to oxidative stress in human skin cells, *Mol. Cell* 59 (2015), <https://doi.org/10.1016/j.molcel.2015.06.017>.
- [36] A.P. Gasch, M. Huang, S. Metzner, D. Botstein, S.J. Elledge, P.O. Brown, Genomic expression responses to DNA-damaging agents and the regulatory role of the yeast ATR Homolog Mec1p, *Mol. Biol. Cell* (2001), <https://doi.org/10.1091/mbc.12.10.2987>.
- [37] E.J. Jaehnig, D. Kuo, H. Hombauer, T.G. Ideker, R.D. Kolodner, Checkpoint kinases regulate a global network of transcription factors in response to DNA damage, *Cell Rep.* (2013), <https://doi.org/10.1016/j.celrep.2013.05.041>.
- [38] P. Bu, S. Nagar, M. Bhagwat, P. Kaur, A. Shah, J. Zeng, I. Vancurova, A. Vancura, DNA damage response activates respiration and thereby enlarges dNTP pools to promote cell survival in budding yeast, *J. Biol. Chem.* (2019), <https://doi.org/10.1074/jbc.RA118.007266>.
- [39] L. Qin, M. Fan, D. Candas, G. Jiang, S. Papadopoulos, L. Tian, G. Woloschak, D.J. Grdina, J.J.J. Li, CDK1 enhances mitochondrial bioenergetics for radiation-induced DNA repair, *Cell Rep.* (2015), <https://doi.org/10.1016/j.celrep.2015.11.015>.
- [40] P. Bai, L. Nagy, T. Fodor, L. Liaudet, P. Pacher, Poly(ADP-ribose) polymerases as modulators of mitochondrial activity, *Trends Endocrinol. Metabol.* (2015), <https://doi.org/10.1016/j.tem.2014.11.003>.
- [41] T.M. Dawson, V.L. Dawson, Mitochondrial mechanisms of neuronal cell death: potential the rapapeutics, *Annu. Rev. Pharmacol. Toxicol.* 57 (2017) 437–454, <https://doi.org/10.1146/annurev-pharmtox-010716-105001>.
- [42] K. Smolková, L. Plecítá-Hlavatá, N. Bellance, G. Benard, R. Rossignol, P. Ježek, Waves of gene regulation suppress and then restore oxidative phosphorylation in cancer cells, *Int. J. Biochem. Cell Biol.* (2011), <https://doi.org/10.1016/j.biocel.2010.05.003>.
- [43] P.S. Ward, C.B. Thompson, Metabolic reprogramming: a cancer hallmark even warburg did not anticipate, *Cancer Cell* (2012), <https://doi.org/10.1016/j.ccr.2012.02.014>.
- [44] D.R. Wise, R.J. DeBerardinis, A. Mancuso, N. Sayed, X.Y. Zhang, H.K. Pfeiffer, I. Nissim, E. Daikhin, M. Yudkoff, S.B. McMahon, C.B. Thompson, Myc regulates a transcriptional program that stimulates mitochondrial glutaminolysis and leads to glutamine addiction, *Proc. Natl. Acad. Sci. U.S.A.* (2008), <https://doi.org/10.1073/pnas.0810199105>.
- [45] R.J. DeBerardinis, A. Mancuso, E. Daikhin, I. Nissim, M. Yudkoff, S. Wehrli, C. B. Thompson, Beyond aerobic glycolysis: transformed cells can engage in glutamine metabolism that exceeds the requirement for protein and nucleotide synthesis, *Proc. Natl. Acad. Sci. U.S.A.* (2007), <https://doi.org/10.1073/pnas.0709747104>.

- [46] C. Jose, N. Bellance, R. Rossignol, Choosing between glycolysis and oxidative phosphorylation: a tumor's dilemma? *Biochim. Biophys. Acta Bioenerg.* (2011) <https://doi.org/10.1016/j.bbabi.2010.10.012>.
- [47] L. Galluzzi, O. Kepp, M.G.V. Heiden, G. Kroemer, Metabolic targets for cancer therapy, *Nat. Rev. Drug Discov.* 12 (2013) 829–846, <https://doi.org/10.1038/nrd4145>.
- [48] F.M. Yakes, B. Van Houten, Mitochondrial DNA damage is more extensive and persists longer than nuclear DNA damage in human cells following oxidative stress, *Proc. Natl. Acad. Sci. U.S.A.* (1997), <https://doi.org/10.1073/pnas.94.2.514>.
- [49] K. Kawamura, F. Qi, J. Kobayashi, Potential relationship between the biological effects of low-dose irradiation and mitochondrial ROS production, *J. Radiat. Res.* (2018), <https://doi.org/10.1093/jrr/rrx091>.
- [50] A. Emadi, S.A. Jun, T. Tsukamoto, A.T. Fathi, M.D. Minden, C.V. Dang, Inhibition of glutaminase selectively suppresses the growth of primary acute myeloid leukemia cells with IDH mutations, *Exp. Hematol.* (2014), <https://doi.org/10.1016/j.exphem.2013.12.001>.
- [51] M.J. Seltzer, B.D. Bennett, A.D. Joshi, P. Gao, A.G. Thomas, D.V. Ferraris, T. Tsukamoto, C.J. Rojas, B.S. Slusher, J.D. Rabinowitz, C.V. Dang, G.J. Riggins, Inhibition of glutaminase preferentially slows growth of glioma cells with mutant IDH1, *Cancer Res.* (2010), <https://doi.org/10.1158/0008-5472.CAN-10-1666>.
- [52] N.D. Amoedo, S. Sarlak, E. Obre, P. Esteves, H. Bégueret, Y. Kieffer, B. Rousseau, A. Dupis, J. Izotte, N. Bellance, L. Dard, I. Redonnet-Vernhet, G. Punzi, M. F. Rodrigues, E. Dumon, W. Mafhouf, V. Guyonnet-Dupérat, L. Gales, T. Palama, F. Bellvert, N. Dugot-Senan, S. Claverol, J.M. Baste, D. Lacombe, H.R. Rezvani, C. L. Pierri, F. Mechta-Grigoriou, M. Thumerel, R. Rossignol, Targeting the mitochondrial trifunctional protein restrains tumor growth in oxidative lung carcinomas, *J. Clin. Invest.* (2021), <https://doi.org/10.1172/JCI133081>.